The Journal of Chemical Physics

Quantitative spectroscopic and theoretical study of the optical absorption spectra of H_2O, HOD, and D_2O in the 125–145 nm region

Bing-Ming Cheng, Chao-Yu Chung, Mohammed Bahou, Yuan-Pern Lee, L. C. Lee, Rob van Harrevelt, and Marc C. van Hemert

Citation: The Journal of Chemical Physics **120**, 224 (2004); doi: 10.1063/1.1630304
View online: http://dx.doi.org/10.1063/1.1630304
View Table of Contents: http://scitation.aip.org/content/aip/journal/jcp/120/1?ver=pdfcov
Published by the AIP Publishing

JOURNAL OF CHEMICAL PHYSICS VOLUME 120, NUMBER 1 1 JANUARY 2004

Quantitative spectroscopic and theoretical study of the optical absorption spectra of H_2O, HOD, and D_2O in the 125–145 nm region

Bing-Ming Cheng
National Synchrotron Radiation Research Center, Hsinchu Science-Based Industrial Park, Hsinchu 30077, Taiwan

Chao-Yu Chung, Mohammed Bahou, and Yuan-Pern Lee
Department of Chemistry, National Tsing Hua University, Hsinchu, 30013, Taiwan

L. C. Lee
Department of Electrical and Computer Engineering, San Diego State University, San Diego, California 92182

Rob van Harrevelt
Theoretische Chemie, Technische Universitaet Muenchen, 85747 Garching, Germany

Marc C. van Hemert
Leids Instituut voor Chemisch Onderzoek, Gorlaeus Laboratoria, Universiteit Leiden, Postbus 9502, 2300 RA Leiden, The Netherlands

(Received 20 August 2003; accepted 8 October 2003)

The room temperature absorption spectra of water and its isotopomers D_2O and HOD have been determined in absolute cross section units in the 125 to 145 nm wavelength region using synchrotron radiation. The experimental results for these $\tilde{B}$ band spectra are compared with results from quantum mechanical calculations using accurate diabatic *ab initio* potentials. A Monte Carlo sampling over the initial rotational states of the molecules is applied in order to calculate the cross sections at a temperature of 300 K. The overall rotation of the water molecule is treated exactly. Both for the experimental and for the theoretical spectrum an analysis is made in terms of a component attributed to rapid direct dissociation processes and a component attributed to longer-lived resonances. The agreement between the results from experiment and theory is excellent for H_2O and D_2O. In the case of HOD in the results of theory two more resonances are found at low energy. It is demonstrated that the width of the resonances of 0.04 eV is the result of overlapping and somewhat narrower resonances in the spectra of molecules differing in rotational ground state.

[DOI: 10.1063/1.1630304]

I. INTRODUCTION

The optical absorption spectrum of water in the 8.6–9.9 eV range (145 to 125 nm), the so-called $\tilde{B}$ band, shows a progression of lines superimposed on a broad background continuum. The lines are approximately 0.04 eV wide and 0.1 eV apart. This structure has intrigued experimentalists and theorists alike over the past 50 years. Among the first to give a detailed analysis of their observed absorption spectra of both H_2O and D_2O, were Wang, Felps, and McGlynn.[1] Lacking detailed knowledge of the excited state potential energy surface (PES) they assigned the bands to a progression in the bending vibration on the second excited state PES that originates from the H–H bonding $3a_1$ orbital to a $3s$ Rydberg orbital transition. The observed slight irregularities in the spacing were interpreted as a signature of the occurrence of another excited state related to a nonbonding $1b_1$ to $3s$ transition. The spectra for H_2O and D_2O are largely similar, except for the difference in spacing between the bands; that is, 0.1 eV on the average for H_2O and 0.08 eV for D_2O. Support for the above assignments was found in the similarity of the scaling with the hydrogen/deuterium mass ratio of the intervals in the bending progression of the excited $^2A_1$ ion state that forms the limit of the Rydberg series. The mixing of the $3s$ Rydberg orbital with the dissociative $4a_1$ valence orbital was held responsible for the width of the lines.

In 1980 Segev and Shapiro[2] performed the first full three-dimensional (3D) quantum dynamics calculations for the water photodissociation. In these calculations the two-dimensional (2D) Flouquet–Horsley[3] *ab initio* PES was used for the excited $\tilde{B}$ state, of $^1A_1$ symmetry. According to Segev and Shapiro, all members of the $\tilde{B}$-band progression could be interpreted as resonances on one single PES, while the width of the resonances was the result of excited state vibrations related to a bending motion on the ridge of the PES embedded in the dissociation continuum. Later calculations by Von Dirke *et al.*,[4] using an improved full 3D PES for the $\tilde{B}\,^1A_1$ state,[5] demonstrated that this single surface assignment could not be correct. Their spectrum, calculated deliberately with one single adiabatic PES, consisted of a dense manifold of narrow resonances, rather different from the resonances calculated by Segev and Shapiro and from the experimental spectrum. Also experimental evidence had appeared to show that the interpretation of Segev and Shapiro was too simple. It was seen in photofragmentation studies[6] that the OH fragments were formed both in the ground state $X\,^2\Pi$ and in the excited state $A\,^2\Sigma^-$, a phenomenon indicative of a dissociation process occurring on more than one PES. Finally in 2000 Van Harrevelt and Van Hemert[7] showed that positions and widths of the peaks in the progression could be reproduced in quantum dynamics calculations when nonadiabatic interactions between the excited $^1A_1$ state and the ground state of the same symmetry were taken into account. In that work it was made clear that the resonances in the calculated spectrum correspond, at least in a 2D reduced dimensionality analysis, to combined bend-stretch motions. Due to the complexity of the calculations, initially only water in the lowest rotational state, $J=0$, was considered. When very recently also the effect of room temperature of the sample was taken into account, i.e., when rotational states with J and K values up to 10 were considered, the amplitudes of the resonances could be reproduced much better than in the $J=0$ only calculations.[8]

A further test of the interpretation of the spectrum, as given by Van Harrevelt and Van Hemert,[8] would be a comparison of the experimental and theoretical spectra for the isotopomers. Such a check had been successfully performed for the rovibrational distributions of the OH/OD fragments resulting in the case of H_2O/D_2O $\tilde{B}$-state photodissociation, both in the $X\,^2\Pi$ ground and in the $A\,^2\Sigma^+$ excited fragment state.[9] Here the experimental data to compare with were only limited to about 10 different wavelengths in the 125–135 nm interval. For the absorption spectra, the absolute absorption cross sections for both H_2O (Refs. 10 and 11) and D_2O (Ref. 10) in the 125 to 145 nm wavelength region were known, but there are as yet no data for HOD. In this paper we report the absorption spectra of H_2O, D_2O, and HOD, in absolute cross section units, as they have been obtained at the National Synchrotron Radiation Research Center (NSRRC) in Taiwan. We confront these new spectra with the results of quantum dynamics calculations performed for these two isotopomers along the same lines as for water as reported in Ref. 8.

In the language of classical trajectories, the broad background continuum can be thought of as resulting from trajectories that lead to rapid, within about 10 femtoseconds (fs), dissociation, while the resonances correspond to indirect trajectories on the coupled surfaces.[12] To visualize this bimodal dissociation character, we transform the experimental spectra to the time domain. In this manner the equivalent is obtained from the autocorrelation function that is used in the theoretical, time-dependent wave packet, formalism. Both the experimental and the theoretical autocorrelation functions are then transformed back over a short time interval sufficient for direct dissociation to obtain only the direct component of the spectrum. The resonant part of the spectrum is found as the difference between the direct spectrum and the full spectrum. In the theoretical studies the full spectrum is calculated from the 100 fs long autocorrelation function.

II. EXPERIMENTAL PROCEDURE

The experimental setup has been described previously.[13,14] In short, VUV light from a high-flux beam line at the NSRRC in Taiwan was dispersed with a 6 m monochromator. The wavelength of the monochromator was calibrated against absorption features of CO (Refs. 15 and 16) and O_2 (Ref. 17). A grating with 600 grooves/mm was used to cover the spectral range 65–250 nm. The slit width was typically 0.05 mm, corresponding to a spectral bandwidth ~0.02 nm. The wavelength uncertainty is estimated to be ±0.02 nm, corresponding to one step of a monochromator scan.

The absorption cross section was measured with a double-beam apparatus.[18] LiF windows transmitting light of $\lambda > 105$ nm served to seal the gas cell. The intensity of the VUV light was monitored with light reflected from a LiF window placed before the gas cell and at 45° from the beam line; the VUV light was converted to visible light with sodium salicylate coated on a glass window, and subsequently detected by a photomultiplier tube (Hamamatsu R943-02). The VUV light transmitted through the gas cell (inner diameter 39.5 mm and path length 8.9 cm) was detected similarly. To avoid variation in pressure due to irradiation or interference from surface absorption or desorption, a reservoir of 1382 cm^3 in volume was connected to the absorption cell.

The absorption cross section σ is evaluated with the equation,

$$\ln(I_0/I) = n\sigma l + A_0,$$

in which I and I_0 are intensities of transmitted and reflected beams, respectively, n is the gas density, $l=8.9$ cm is the path length of the absorption cell, and A_0 is a proportionality factor determined from I and I_0 when the cell was evacuated to less than 5×10^{-7} Torr. At each wavelength, the absorption cross section was obtained on fitting with linear least-squares 8–14 absorbance values measured at various pressures; the uncertainty is estimated to be 5%. The pressure of the absorbing gas was selected in the range 0.04–10.2 Torr, so as to limit absorbance to be less than 2 to avoid saturation effects. The gas density at room temperature was determined from gas pressure, which was monitored with a MKS-Baratron pressure meter.

Gas vapors were obtained from pure liquid samples of H_2O and D_2O (Merck Sharp and Dome, isotopic purity 99.8%). HOD was prepared from a mixture of deionized H_2O and pure D_2O with a molar ratio 1:2.806. For experiments involving deuterated samples at least ten cycles of passivation were carried out. Relative concentrations of H_2O, D_2O, and HOD in the gas sample mixture were determined from the equilibrium constant for

$$H_2O_{(l)} + D_2O_{(l)} \rightleftarrows 2\,HOD_{(l)}$$

which is $k_{eq}=3.74\pm0.02$ (at 298 K).[19,20] The molar fractions of gaseous H_2O, HOD, and D_2O of this sample are determined to be 0.079, 0.395, 0.526. For samples of mixed isotopic species, absorption cross sections of H_2O and D_2O measured in this work were subtracted from the observed spectrum to derive a spectrum of HOD.

The cross section σ is decomposed into a diffuse background component, σ_{dir}, and a modulating indirect component, $\sigma_{indir} = \sigma - \sigma_{dir}$. σ_{dir} is determined by smoothing an observed spectrum into a continuous profile; this smoothing results from removing Fourier components with frequencies greater than $1/(100\ \Delta n)$, in which Δn is the abscissa spacing of data points. The function used to eliminate the high-frequency components is a parabola with its maximum at zero frequency, decaying to zero at the cutoff frequency defined above.

III. QUANTUM DYNAMICS CALCULATION PROCEDURE

The procedure for calculating cross sections of water with nonzero angular momentum has been described in detail previously.[8] Here we summarize the procedure for H_2O. With a Monte Carlo sampling a representative 300 K ensemble of water molecules in different rotational states is generated. The different statistical weights for ortho and para species are taken into account. For each rotational state, $(J,\ K)$, where J is the total angular momentum and K labels the $2J+1$ sublevels, a separate cross section calculation is performed.

The time-dependent wave packet formalism is used where the wave function is expanded in rotoelectronic basis functions.[21] This is a convenient manner to account for coupling between electronic states due to nonadiabatic interaction and rotation of a molecule. The wave packets are propagated on three coupled diabatic surfaces during a time span of 76.8 fs. For HOD and D_2O, the same procedure has been applied. Also for D_2O, the appropriate weight factors for ortho and para levels have been taken into account. As required by the slower dynamics of the heavier D atoms, a longer propagation time is applied (105.6 fs).

The potential energy surfaces and the couplings are copied from Ref. 22. The wave packets at time zero are obtained by multiplying the wave function for the $(J,\ K)$ ground state with the appropriate electronic transition dipole moment functions taken from Ref. 23. For D_2O and HOD the grid spacing has been decreased from 0.12 to 0.09 Bohr, and the size of the basis set used in the rotational kinetic energy operation has been increased from $j_{\max}=60$ to $j_{\max}=80$. For each selected $(J,\ K)$, separate calculations with $\Delta J=-1$, 0, and 1 are performed. For each $(J,\ K,\ \Delta J)$, the cross section is obtained from the Fourier transform of the autocorrelation function of the time-dependent wave function. The full spectrum is obtained by averaging the $(J,\ K,\ \Delta J)$ contributions.

In order to facilitate the study of the resonances, the cross section σ is decomposed into a diffuse background part, σ_{dir}, and an indirect part, σ_{ind}, as was done for the experimental spectrum. The direct part is also computed from the autocorrelation function, but now truncated before the first recurrence time, i.e., at 12 fs. This decomposition scheme is applied both for the full summed spectrum, and for individual $(J,\ K)$ contributions.

In our previous study for water we used 17 rotational states in the Boltzmann average, and there the statistical error in the cross section was always less than 5% and 2% on the average, for the energy range considered (8.6–9.9 eV). It appears that for 12 rotational states the average is hardly different from the 17 states average. The statistical error is then 5% on the average, and always smaller than 10%.

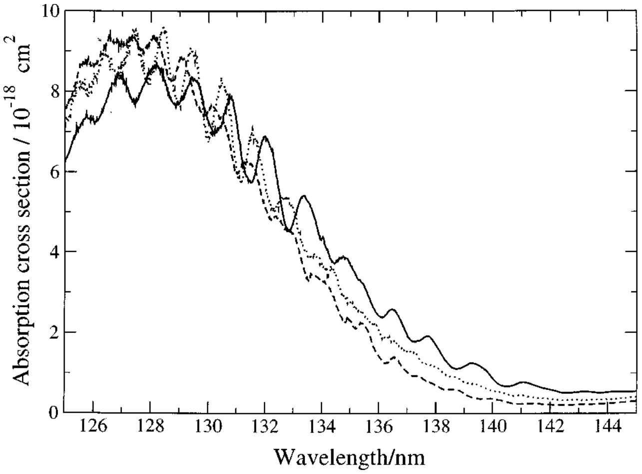

FIG. 1. Experimental absorption cross sections of H_2O (full line), HOD (dotted line), and D_2O (dashed line) in the spectral region 125–145 nm (8.6–9.9 eV).

IV. RESULTS AND DISCUSSION

Experimental absorption cross sections of H_2O, HOD, and D_2O in the spectral region 125–145 nm (8.6–9.9 eV) are shown in Fig. 1. Cross sections at 1 nm intervals for each species are listed in Table I; a complete listing of data at 0.02 nm intervals is available through internet at http://ams-bmc.nsrrc.org.tw. Cross sections of H_2O determined in this work are in good agreement with those of Lee and Suto[10] and Yoshino *et al.*;[11] however, they are lower than those reported by Chan *et al.*[24] by about 30%. Cross sections of D_2O determined in this work are in good agreement with those of Lee and Suto.[10] No absorption cross sections of HOD in this spectral region have been reported previously.

In Fig. 2 the indirect spectrum derived from the present experimental spectrum is compared with the indirect spec-

TABLE I. Absorption cross sections (in units of 10^{-18} cm^2) of water isotopomers in the 125–145 nm region.

Wavelength/nm	H_2O	D_2O	HOD
145	0.55	0.30	
144	0.53	0.24	0.35
143	0.53	0.22	0.34
142	0.59	0.22	0.36
141	0.77	0.24	0.45
140	0.88	0.36	0.56
139	1.17	0.50	0.79
138	1.69	0.70	1.14
137	1.94	1.03	1.52
136	2.42	1.43	2.07
135	3.67	2.30	2.76
134	4.36	3.30	3.61
133	4.82	4.44	5.05
132	6.89	5.11	5.73
131	7.19	5.96	5.97
130	7.19	7.56	6.94
129	7.74	8.77	7.69
128	8.56	9.29	8.50
127	8.39	9.20	8.58
126	7.24	8.62	8.46
125	6.30	7.58	7.29

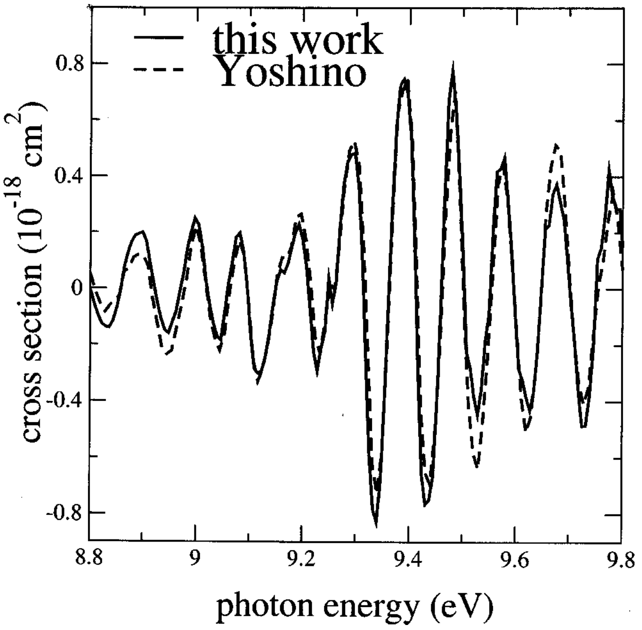

FIG. 2. The indirect spectrum of H_2O derived from the present experimental spectrum as compared with the indirect spectrum derived from the spectrum of Yoshino *et al.* (Ref. 11).

trum derived from Yoshino's spectrum.[11] The agreement with respect to resonance positions is excellent. The small differences in amplitudes might be due to experimental uncertainties. Also the finer details that were sometimes attributed to noise appear in both spectra.

In Fig. 3 the convergence of the theoretical cross sections with the number of rotational states present in the Boltzmann averaging procedure is shown for the indirect part of the cross section for each of the three isotopomers. Taking more than 12 rotational states would probably change only minor details in the spectra of HOD and D_2O, thus we expect that the main features will remain the same. The convergence is faster for H_2O than for HOD and D_2O. Figure 3 also underlines that the main effect of the averaging process is a washing out of the resonance structures, as has been discussed before.

Next, in Figs. 4(a)–4(c) the total cross sections from the experiments are compared with those from theory. Both the experimental and the theoretical spectra show that the general structure of the spectrum is similar for the three isotopomers. The most obvious difference concerns the width of the band: going from H_2O via HOD to D_2O, the ground state vibrational wave function becomes narrower, and this is reflected in the smaller bandwidth. The agreement between the experimental and theoretical direct spectra (not shown) is striking: the experimental values of the energy at half of the maximum are 9.24 eV for H_2O and 9.35 eV for D_2O, while the theoretical are 9.26 and 9.37 eV, respectively. The theoretical direct spectrum for HOD is again found at only 0.02 eV higher energy values than the experimental spectrum. The good agreement between theoretical and experimental direct cross sections implies that the potential energy surface is very accurate in the Franck–Condon region. Also the absolute values of the cross sections are well reproduced, which implies that the calculated transition dipole moment surface is accurate. At energies above 9.6 eV the direct theoretical spectra start to deviate from the experimental spectra, because the calculated transition dipole moment also contains a contribution of the bound $\tilde{D}$ state for geometries where the potential energy is high.[23]

The indirect cross section depends on a range of the potential energy surface much larger than for the direct cross section. In Ref. 7, the nature of the resonances has been investigated. Here, the results of that analysis are briefly summarized. The main characteristics of the resonance structure in the spectrum can be explained by a simple two-dimensional model, in which one OH distance is fixed, and in which only dynamics on the adiabatic $\tilde{B}$ potential energy surface is considered. This surface has two minima, one for the collinear HOH geometry, and one for the collinear HHO

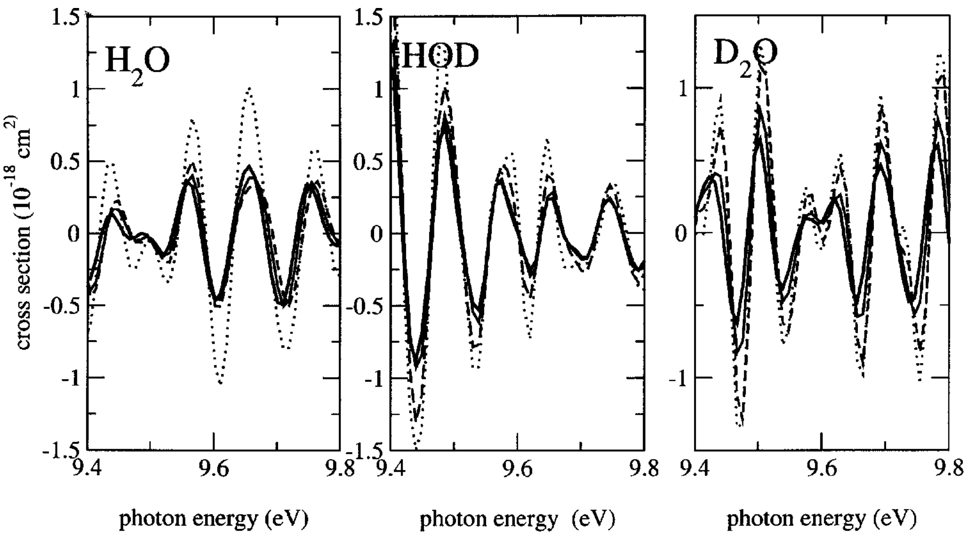

FIG. 3. The convergence of the cross sections with the number of rotational states, N_{rot}, present in the Boltzmann averaging procedure as shown for the indirect part of the cross section for each of the three isotopomers. Thick line is the result for 12 rotational states. The thin lines are average cross sections for N_{rot} values of 1 (dotted line), 4 (dashed line), and 8 (full line).

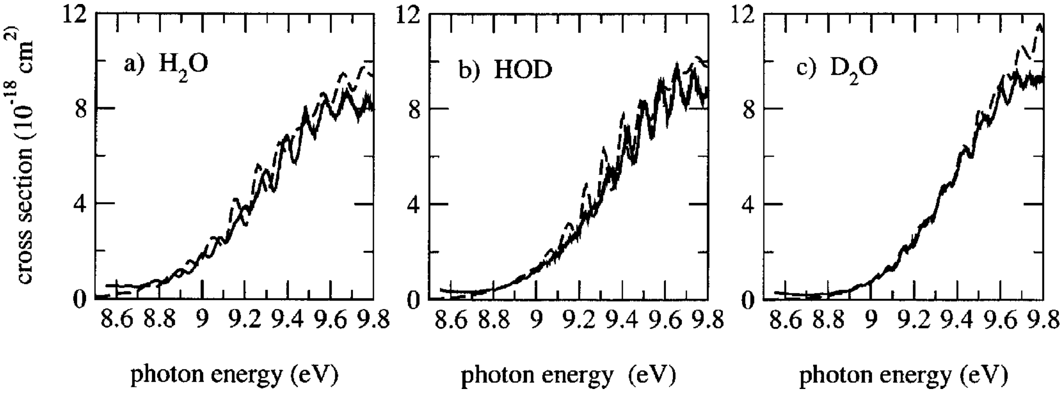

FIG. 4. Comparison of the total cross sections from the experiments (drawn curves) with those from theory (dashed curves). Panel (a) for H_2O, panel (b) for D_2O, and panel (c) for HOD.

geometry. For both minima the distance between OH and H is large $(3-4a_0)$. The wave packet initially moves directly to the HOH minimum. Here, the OH–H distance is so large $(3a_0)$, that one can consider one OH bond to be almost broken. The largest part of the wave packet moves further towards the asymptotic OH+H region, another part moves towards the HHO geometry. The excitation of the bending motion is so high that rotational barriers prevent a rapid dissociation process for this part of the wave packet, which is thus trapped in long-lived resonances. The bifurcation of the wave packet has been described by Dixon *et al.*[25] in a calculation of the photodissociation dynamics at 10.2 eV.

The nature of the resonances depends on energy. Below 9 eV, the resonances found in the spectrum correspond to resonances in the HOH well, and can roughly be described by bending and stretching quantum numbers. For energies higher than the barrier between the HOH and HHO wells, the resonances are very complicated, and show tunneling behavior between the two minima. When the energy is significantly above the barrier, the resonances look simple again. In a classical description, the H atom makes a complete circle around the OH molecule, while the distance to OH varies, but is most of the time large $(3-4a_0)$. The spectrum shows a rather regular progression over the entire energy range, even though the nature of the resonances changes. The spectrum of D_2O is found to be similar to that of H_2O (Ref. 7) with a spacing of 0.08 eV instead of 0.10 eV. This is explained by the mass difference between D and H, the ratio is slightly larger than $\sqrt{2}$.

In Figs. 5(a)–5(c), the new experimental and theoretical indirect cross sections are shown for H_2O, HOD and D_2O. All indirect cross sections show a regular progression with a spacing of 0.10 for H_2O, and 0.08 eV for HOD and D_2O. The agreement between experimental and theoretical spacings is very good. When the spectra of H_2O, HOD, and D_2O are overlaid, both the experimental and the computed ones, it is seen that the HOD spectrum resembles the D_2O spectrum more than the H_2O spectrum. This can be understood by noting that in HOD the dissociation towards OD+H is four times as probable as the dissociation into OH+D, because the OH bond is weaker. What are seen in the spectrum of HOD are sums of resonances in combined stretch-bend modes of OD and departing H. Since the bending mode is dominant, it can be expected that the spacing between the resonances correlate with the reduced mass of the bending mode. The reduced mass for the bending mode of the OD–H complex with H far away is close to that of the OD–D complex.

Also for the amplitudes of the resonances, the agreement between theory and experiment is good, for all isotopomers. A striking feature of the D_2O spectrum is that the amplitude of the modulation is almost a factor of 2 smaller than for

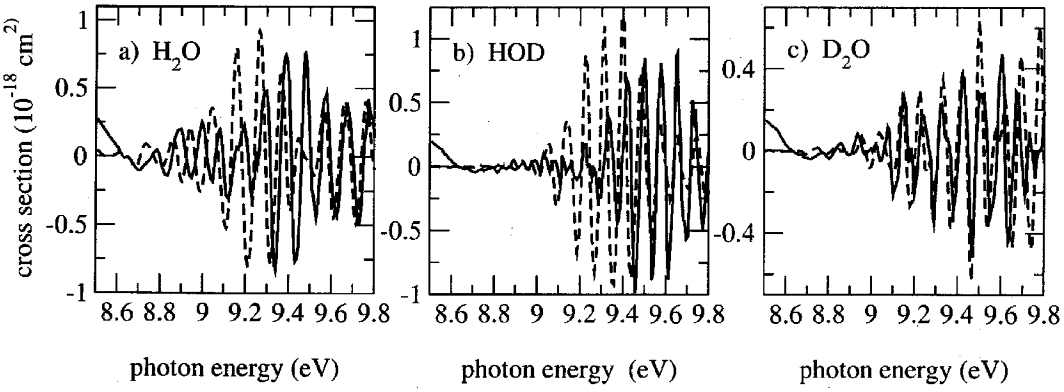

FIG. 5. Comparison of the indirect cross sections from the experiments (drawn curves) with those from theory (dashed curves). Panel (a) for H_2O, panel (b) for D_2O, and panel (c) for HOD.

H_2O. This is also the case for cross sections for individual rotational states. An explanation is that the resonances in the spectra are already partially overlapping. For D_2O, for which the resonances are closer to each other, the overlapping is stronger than for H_2O, which leads to a reduced indirect cross section. But the same argument apparently does not hold for HOD: For HOD the indirect cross section is even a bit larger than that of H_2O, both experimentally and theoretically.

There is only one feature for which experiment and theory disagree: for HOD the onset of the resonances occurs at lower energy in the theoretical spectrum than in the experimental spectrum. The experimentally observed trend in the onsets of the resonances, first H_2O, then D_2O and HOD last, is however reproduced by theory. For H_2O and D_2O the onset of the resonances is seen to be hardly different in theory and experiment. In the case of HOD theory predicts two low energy resonances that are not present in the experimental spectrum; also the amplitude of the next resonances is higher in theory than in experiment.

In summary, good agreement between experiment and theory is found for H_2O and D_2O, but for HOD a large discrepancy in the onset of the resonances has been found. Since agreement between the theoretical and experimental direct spectra is excellent, one might jump to the conclusion that the direct dissociation process is well described, but that the indirect dissociation process where larger parts of the potential energy surfaces are sampled still requires improvement. Along what lines is as yet not clear. That the only disagreement is found for HOD and not for H_2O and D_2O suggests that the potential does not describe adequately symmetry effects. The energy of 9.3 eV, where the resonances appear in the experimental HOD spectrum, corresponds roughly to the energy of the barrier between the HOD and HDO regions. Resonances below 9.3 eV correspond to large amplitude stretch–bend vibrations, and those above 9.3 eV to more complicated orbital involving a rotation of the departing H around OD. It could be that especially the low energy stretch–bend modes are sensitive to symmetry effects that are not well described by the current potential energy surfaces and couplings.

V. CONCLUDING REMARKS AND SUMMARY

The photodissociation cross sections for H_2O, D_2O and a mixture of H_2O and D_2O were measured in the 125–145 nm, $\tilde{B}$ band, region. Synchrotron radiation was used. The spectra of the pure isotopomers are in accord with the most accurate previous measurements, the mixture enables the derivation of the HOD cross section for the first time. Quantum mechanical calculations are performed for all three isotopomers. In the wave packet calculations the effect of a temperature of 300 K of the samples is accounted for by explicitly including molecular rotation. The nonadiabatic coupling between the second excited state and the ground state is taken into account by the use of accurate *ab initio* diabatic potentials. The experimental spectra are decomposed into components corresponding to a fast, direct dissociation process and a process proceeding through resonances by transforming to and from the time domain. In this way a detailed comparison is made with the theoretical results where an analogous separation into direct and resonant contributions is made through manipulation of the autocorrelation function. The direct experimental and theoretical spectra are seen to be nearly identical, indicative of high accuracy in the part of the potential energy surface related to direct dissociation. Also the experimental and theoretical resonances show nice agreement, both in position and in width, at least for H_2O and D_2O. The width of the resonances, that are 0.10 eV apart for H_2O and 0.08 eV for D_2O, amounts to 0.04 eV and is the consequence of overlapping resonances in the spectra of molecules having different ground state rotational levels. It is therefore expected that at still higher temperature the water $\tilde{B}$ band absorption spectrum will be even more less structured, while it should be possible to detect narrower resonances in cold beams. For HOD the resonant component of the theoretical spectrum shows two resonances at low energy that are not seen in the experimental spectrum. On the origin of this unexpected discrepancy we can only speculate.

[1] H. T. Wang, W. S. Felps, and S. P. Mc Glynn, J. Chem. Phys. **67**, 2614 (1977).
[2] E. Segev and M. Shapiro, J. Chem. Phys. **77**, 5604 (1982).
[3] F. Flouquet and J. A. Horsley, J. Chem. Phys. **60**, 3767 (1974).
[4] M. Von Dirke, B. Heumann, K. Kuehl, T. Schroeder, and R. Schinke, J. Chem. Phys. **101**, 2051 (1994).
[5] B. Heumann, K. Kuehl, K. Weide, R. Dueren, B. Hess, U. Meier, and S. D. Peyerimhoff, Chem. Phys. Lett. **166**, 385 (1990).
[6] K. Mordaunt, M. N. R. Ashfold, and R. Dixon, J. Chem. Phys. **100**, 7360 (1994).
[7] R. Van Harrevelt and M. C. Van Hemert, J. Chem. Phys. **112**, 5787 (2000).
[8] R. Van Harrevelt and M. C. Van Hemert, Chem. Phys. Lett. **371**, 701 (2003).
[9] J. H. Fillion, R. van Harrevelt, J. Ruiz, N. Castillejo, A. H. Zanganeh, J. L. Lemaire, M. C. van Hemert, and F. Rostas, J. Phys. Chem. A **105**, 11414 (2001).
[10] L. C. Lee and M. Suto, Chem. Phys. **110**, 161 (1986).
[11] K. Yoshino, J. R. Esmond, W. H. Parkinson, K. Ito, and T. Matsui, Chem. Phys. **211**, 387 (1996).
[12] R. Van Harrevelt, M. C. Van Hemert, and G. C. Schatz, J. Phys. Chem. A **105**, 11480 (2001).
[13] B.-M. Cheng, E. P. Chew, C.-P. Liu, M. Bahou, Y.-P. Lee, Y. L. Yung, and M. F. Gerstell, Geophys. Res. Lett. **26**, 3657 (1999).
[14] B.-M. Cheng, C.-Y. Chung, M. Bahou, Y.-P. Lee, and L. C. Lee, J. Chem. Phys. **117**, 4293 (2002).
[15] S. G. Tilford, J. T. Vanderslice, and P. G. Wilkinson, Can. J. Phys. **43**, 450 (1965).
[16] J. D. Simmons, A. M. Bass, and S. G. Tilford, Astrophys. J. **155**, 345 (1969).
[17] S. Ogawa and M. Ogawa, Can. J. Phys. **53**, 1845 (1975).
[18] C.-Y. Chung, E. P. Chew, B.-M. Cheng, M. Bahou, and Y.-P. Lee, Nucl. Instrum. Methods Phys. Res. A **467–468**, 1572 (2001).
[19] J. W. Pyper, R. S. Newbury, and G. W. Barton, Jr., J. Chem. Phys. **46**, 2253 (1967).
[20] I. Kirshenbaum, in *Physical Properties and Analysis of Heavy Water*, edited by H. C. Urey and G. M. Murphy (McGraw-Hill, New York, 1951).
[21] G. G. Balint-Kurti and M. Shapiro, Chem. Phys. **61**, 137 (1981).
[22] A. J. Dobbyn and P. J. Knowles (unpublished).
[23] R. Van Harrevelt and M. C. Van Hemert, J. Chem. Phys. **112**, 5777 (2000).
[24] W. F. Chan, G. Cooper, and C. E. Brion, Chem. Phys. **178**, 387 (1993).
[25] R. N. Dixon, D. W. Huang, X. F. Yang, S. Harich, J. J. Lin, and X. Yang, Science **285**, 1249 (1999).